ELSEVIER

Contents lists available at ScienceDirect

Journal of the Energy Institute

journal homepage: www.elsevier.com/locate/joei





A single-step upcycling of PVC-containing municipal solid waste compositions for greener chemicals and clean solids as fuel or oil absorbent

Xiaolin Chen¹, Xianglan Bai *

Department of Mechanical Engineering, Iowa State University, Ames, IA, USA

ARTICLE INFO

Keywords: Cellulose Polyvinyl chloride Plastics Levoglucosan Furfural Absorbent

ABSTRACT

Polyvinyl chloride (PVC) containing municipal solid waste (MSW) streams are difficult to recycle and mostly landfilled due to various detrimental effects PVC causes to waste recycling. In this work, a single-step upcycling of PVC-containing commingled wastes in tetrahydrofuran was investigated using cellulose, PVC, polyethylene (PE), polypropylene (PP), and polystyrene (PS) to model the wastes. During the co-conversion, *in-situ* produced HCl derived from PVC decomposition acted as an acid catalyst to selectively decompose cellulose into liquid mainly containing levoglucosan (LGA) and furfural. It was also found that the presence of PE, PP, and PS in the mixture synergistically enhanced the cellulose-derived monomer productions and increased the reaction rate for producing the monomers by suppressing secondary reactions of HCl in the solvent. The maximum LGA yield from co-conversion of cellulose, PVC, and PS was 35.4% after a 5 min reaction compared to the 31.7% obtained without PS in the mixture. In addition to converting cellulose to chemicals, PVC-derived polyaromatics and partly decomposed PE, PP, and PS were recovered as solids. The dechlorinated solids had higher heating values up to 46.11 MJ/kg, achieved by co-converting cellulose, PVC, and PP. When used as oil absorbents in water, the solid recovered from converting cellulose, PVC, and PE mixture showed the highest absorption capability. Overall, the presented approach offers a promising way for upcycling PVC-containing wastes in which PVC properties and its molecular structure are leveraged to enhance the conversion.

1. Introduction

In 2019, 368 million tons of plastics were produced worldwide [1]. Due to the notable advantages, such as low cost, moldability, durability, resistance to corrosion, and poor conduction of heat and electricity, the global demand for plastic products continues to grow. Global plastic production increases at an annual rate of approximately 8.4%, and the amount is estimated to reach 500 million tons in 2025 [2-5]. It is reported that among the 8.3 billion tons of virgin plastics produced so far. 6.3 billion tons became end-of-life plastics between 1950 and 2015. Of the plastic waste, 12% was incinerated, and 79% ended up in landfills or the natural environment [6]. It is estimated that, by 2050, approximately 12 billion tons of plastic waste will be disposed of in landfills or the natural environment. Plastic wastes can remain in landfills for decades to hundreds of years due to their slow degradation [7,8]. Landfilled plastics can generate toxic substances to contaminate underground water and deteriorate the surrounding lands [9]. Compared to presorted waste plastics, commingled municipal solid wastes (MSW) containing both plastics and organic materials are much more difficult to manage due to their heterogeneous and high contaminant composition.

Commonly used methods for recycling commingled solid wastes include incineration, pyrolysis, and gasification. Although incineration of MSW can recover energy, it causes air pollution and acidic rains due to the release of toxic gases, which are detrimental to vegetation, animal and human health, and the environment as a whole [10]. While the pyrolysis of MSW produces a storable oil product, the oil with complex composition requires subsequent upgrading to become fuels or chemicals. Gasification, on the other hand, produces syngas. Besides the high energy requirement for gasification, syngas cleaning is also challenging. Among all the wastes considered for recycling, PVC and PVC-containing wastes are the most difficult to recycle. PVC, which makes up 10% of total plastic waste, is the major halogen source in MSW [11]. Thus, PVC in the waste streams is strongly undesired and must be avoided in most recycling approaches. The chlorinated dioxins liberated during PVC combustion can cause cancer and irreversible neurological damage [12, 13]. Hydrogen chloride (HCl) gas released from PVC decomposition can

E-mail address: bxl9801@iastate.edu (X. Bai).

^{*} Corresponding author.

¹ Current address: Catalytic Carbon Transformation and Scale-up Center, National Renewable Energy Laboratory, Golden, CO 80401, USA.

cause acid rain and climate change [14]. Mechanical recycling of PVC is limited due to its low thermal stability compared to other common plastics, the various additives added to PVC, and the low quality of PVC [15]. Not only does PVC produce toxic halogens when combusted or pyrolyzed [16,17], but it also negatively impacts the chemical recycling of PVC-containing waste streams. For example, the presence of PVC increases char formation from other plastics during their co-pyrolysis [18]. PVC also promotes undesired char and water products from organic compositions [19–21], producing chorine-contaminated char [22] and chlorinated oil compounds [21] upon pyrolysis. PVC also has a strong catalyst poisoning effect, reducing tar cracking efficiency during co-gasification with other MSW compositions [23].

Various dechlorination strategies of PVC-containing wastes have been studied [21,24]. For example, PVC-containing wastes were torrefied to remove HCl, or the pyrolysis vapor of the PVC-containing waste materials was neutralized using base solutions [19,25,26]. Since HCl is water soluble, hydrothermal treatment of PVC-containing wastes gained increasing attention [27,28]. Upon hydrothermal treatments, hydrothermal char with a low chlorine content was used as a combustion fuel or further pyrolyzed for oil [29,30]. This method was used to convert PVC mixed with other plastics [31] or PVC mixtures with various organic wastes [32-36]. However, these products usually have low economic value, and post-treating contaminated wastewater creates an additional burden. Furthermore, obtaining completely dechlorinated solids or oils is usually difficult, potentially causing secondary contaminations when the products are applied. Due to a lack of efficient methods for recycling PVC, PVC-containing waste streams are currently discarded in landfills. Moving forward, developing efficient waste upcycling to minimize the detrimental effects caused by PVC content in the mixture and improving the economic values of recycled products is necessary.

In this context, our previous study shows that co-converting PVC and biomass in polar aprotic solvents could utilize PVC as a resource rather than a burden to produce value-added products [37,38]. We found that during their co-conversion in polar aprotic solvents, PVC can decompose ahead of biomass to release HCl, and the solvent-solubilized acid could then serve as an acid catalyst to promote polysaccharide depolymerization to valuable monomers [37]. Choosing a polar aprotic solvent as a conversion medium was important in this approach. Unlike protic solvents like water and alcohols, polar aprotic solvents do not donate hydrogen atoms. Therefore, hydrolysis reactions do not occur in polar aprotic solvents. However, polar aprotic solvents can greatly amplify acid-catalyzed reactions by affecting the stability of the acidic proton relative to protonated transition states [39,40]. Polar aprotic solvents could also promote the depolymerization of polysaccharides by lowering the activation energy for glycosidic chain cleavage, while their exquisite solvation capability could dissolve depolymerized products [41]. As a result, we observed that PVC-derived HCl, even at very low concentrations, could dramatically enhance the depolymerization of polysaccharides to anhydrosugar monomers [37]. We also found that while HCl serves as a catalyst, the polyene or polyaromatics after PVC dechlorination can also react with the lignin fraction of biomass to form clean solid fuels [38]. While our previous results suggest the conversion in polar aprotic solvents to be a potentially attractive solution for PVC-containing waste streams, MSW streams also contain other common plastics besides organic wastes. In this work, we employed cellulose, polyethylene (PE), polypropylene (PP), and polystyrene (PS) as model MSW compositions to evaluate the possibility of extending the above-mentioned approach of PVC conversion to complex co-mingled MSW streams. Cellulose is the most abundant organic composition in MSW and can be found in paper, cardboard, wood, yard wastes, and food wastes. On the other hand, PE, PP, and PS are the most common plastic wastes, accounting for more than 65% of total plastic waste [42]. Tetrahydrofuran (THF) was used as the conversion solvent. It is a low boiling solvent (thus can be easily recovered using low energy) and can be synthesized using biomass-derivable chemicals [43]. The present study showed that PVC-containing co-mingled mixtures could be co-upcycled using a single-step process into high-value green chemicals and clean, versatile solid products. We found that non-PVC plastics in the mixture synergistically enhance PVC-catalyzed cellulose conversion to levoglucosan and furfural. We also found that dechlorinated hydrocarbons of PVC interact with other plastics and cellulose-derived char to form clean and energy-dense solid fuels that could also be used as oil absorbents. Based on the current approach, PVC, organic, and plastic compositions in the mixtures could all be upcycled into versatile value-added products. To our knowledge, no previous studies reported producing similarly high-value products from PVC-containing complex mixture compositions while minimizing secondary contaminant production.

2. Experimental

2.1. Materials

Avicel PH101 cellulose was purchased from Sigma-Aldrich. PVC, high-density PE, PP, and PS powders were purchased from Shanghai Yangli Mechanical and Electrical Technology Co., Ltd, China. HPLC grade THF stabilized with 0.025% butylated hydroxytoluene (BHT) was purchased from Fisher Chemical. Levoglucosan (LGA) and 1,6-anhydro- β -D-glucofuranose (AGF) were also purchased from Fisher Scientific. Furfural (FF), 4-chloro-1-butanol (CB), and Sudan II were purchased from Sigma-Aldrich. Paraffin oil was purchased from Carolina Biological, and canola oil was purchased from the local grocery store.

2.2. Conversion in THF

The conversion in THF solvent was conducted at 285–335 $^{\circ}$ C in Swagelok mini reactors. The reactors assembled by two 1/2-inch plugs and a 1/2-inch port connector had an inner volume of 3 mL. Inside the reactors, 12 mg of cellulose and 12 mg of PE, PP, or PS (1:1 mass ratio) were added to 2 mL of THF. Different amounts (0.75–3 mg) of PVC were added before the reactors were sealed. The reactors were heated by a preheated industrial fluidized sand bath. After conversion, the reactors were removed from the sand bath and cooled in a room-temperature water bath.

The liquid and solid inside the reactor were filtrated for separation. The solid was dried in a vacuum oven overnight at 40 $^{\circ}$ C before being weighed. To determine gas formation, the cooled reactors containing the products and post-reaction solvent were weighted using a Mettler Toledo high-precision analytical balance (accuracy: 0.1 mg) before and after the reactor cap was loosened. The gas yield was negligible even at the highest reactor temperature. The estimated error for gas yield is between 0.3 and 0.8%, determined based on the accuracy of the analytical balance and the feedstock mass inside the reactor. When cellulose was co-converted with PE, PP, and PS in the presence or absence of PVC, the product yields were determined using equations (1) and (2):

Solid yield (%) =
$$\frac{\text{mass of solid}}{\text{total mass of feedstock}}$$
 (1)

Liquid yield (%) =
$$100\%$$
 – solid yield (%) (2)

When cellulose alone or the mixtures of cellulose and PVC were converted, the "calculated" solid yield was reported, which was determined using equation (3):

In equation (3), 12 mg is added, which is the same mass of PE, PP, or PS co-converted with cellulose in this study.

Additionally, PVC was converted with PE, PP, or PS in THF. The

mixtures containing cellulose, PVC, PE, PP, or PS were also converted using deionized water as the solvent. Each test condition was triplicated, and the average values were reported.

2.3. Oil absorption test

The oil absorption test was performed using the literature method [44]. Specifically, 20 mL of oil was dyed red with 0.2 mg of Sudan II and then added to 10 mL of deionized water in a beaker. Approximately 10 mg of the solids recovered from the solvent-based conversion were immersed in the water-oil solution. After 10 min, the solids were dried overnight in a 40 $^{\circ}\text{C}$ vacuum oven. The solid was weighed before and after the absorption to determine the mass of the absorbed oil. The oil absorption capacity was calculated using the equation given below:

Absorption capacity (%) =
$$\frac{\text{mass of absorbed oil}}{\text{solid mass}}$$

2.4. Product characterizations

The methods for the liquid and solid analysis were similar to our previous study [38]. An Agilent 7890B gas chromatograph (GC) with a mass spectrometer (MS) and flame ionization detector (FID) was used for analyzing liquid composition. In the GC, two ZB-1701 (60 m \times 250 $\mu m \times 0.25~\mu m)$ capillary columns were used. In the GC, the oven temperature was held at 40 °C for 3 min and increased to 280 °C with a rate of 4 °C/min. The oven was maintained at the final temperature for an additional 4 min. In the GC/MS, the helium flow rate was 1 mL/min, and a split ratio at the inlet was 20:1. The compounds identified by MS were quantified by FID. Five concentrations of LGA, AGF, FF or CB were injected to GC/MS-FID to create calibration curves.

The solution pH value was determined by a pH meter (Mettler Toledo SevenMulti pH meter).

The oxidative combustion titration method (i.e., Method 9076) was used to determine the chlorine in solids. The complete combustion of the solid was conducted in the sealed apparatus. Subsequently, deionized water was added to the apparatus. As an indicator, a small amount of $\rm K_2CrO_4$ was added to the water solution. AgNO $_3$ was added to the solution dropwise to precipitate chloride ions until the solution color suddenly changed due to the $\rm Ag_2CrO_4$ formation. The total amount of AgNO $_3$ added was used to calculate the chlorine content of the sample. CB, the organic chloride in the reaction solvent, was analyzed using GC/MS

Thermogravimetric analysis (TGA) was conducted using a Mettler Toledo TGA. Approximately 20 mg of solid was heated from room temperature to 900 $^{\circ}\text{C}$ at a heating rate of 10 $^{\circ}\text{C/min}$. The TGA was performed using nitrogen with a flow rate of 100 mL/min.

A Thermo Scientific Nicolet iS10 (Thermo Fisher Scientific) with a Smart iTR accessory was used to perform Fourier-transform infrared spectroscopy (FTIR) analysis. The range of the wavenumbers was from $750~{\rm cm}^{-1}$ to $4000~{\rm cm}^{-1}$.

Fast pyrolysis was performed using a two-stage Frontier tandem micro-pyrolyzer system (Rx-3050 TR, Frontier Laboratory) using helium gas. Each time, approximately 250 μg sample in a deactivated sample cup was dropped into a first-stage pyrolysis oven preheated at 500 $^{\circ} C$. The empty second-stage reactor was maintained at 300 $^{\circ} C$ to avoid condensation of the pyrolytic products. The pyrolytic vapor was analyzed by an online GC/MS-FID.

A CHNS Elemental Analyzer (Vario Micro Cube) was used to determine elemental composition. Carbon, hydrogen, and nitrogen contents in the solid sample were measured by the instrument, and oxygen content was determined by mass difference. Dulong's Formula was used to calculate the higher heating value (HHV)s of the samples.

The microstructures of plastics and the solids were observed using a scanning electron microscope (SEM, Quanta-FEG 250, FEI) and an accelerating voltage of $10\ kV$.

The experimental procedure is summarized in Fig. 1.

3. Results and discussion

3.1. Co-conversion of cellulose and different types of plastics in THF

Cellulose was converted in 310 °C THF alone or co-converted with PE, PP, PS, or PVC. It should be noted that the total feedstock masses vary depending on the mixture contents. To evaluate possible synergistic effects among different feedstock compositions, "calculated" liquid yields were reported by converting cellulose alone or cellulose and PVC mixtures (please see Equation (3) in the experimental method section). The "calculated" yields are the yields that would be obtained if PE, PP, or PS were also presented in the feedstock, but their presence does not affect the conversion of cellulose or the co-conversion of cellulose and PVC. When cellulose was co-converted with a 1:1 mass ratio of PE, PP, or PS (12 mg:12 mg, same in the following tests) without PVC in the mixture, the actual liquid yields were slightly lower than the "calculated" yield (e.g., 12.7%, 12.3%, and 13.5%, respectively, compared to 14.2%). With PVC in the mixture (an 8:1 mass ratio of cellulose and PVC), the significantly higher "calculated" liquid of 48.0% was observed after a shorter time of 10 min. The liquid yield of cellulose and PVC coconversion was much higher than the liquid yields without PVC in the feedstock, implying that PVC strongly promotes the liquefaction of cellulose in the solvent.

The major monomers in the liquid were LGA, FF, and AGF, derived from cellulose. Thus, their yields were reported per the cellulose mass in the feedstock materials. CB was also produced when cellulose and PVC were co-converted, whose formation will be discussed later in this article. The yields of LGA, AGF, and FF as a function of reaction time for different feedstock compositions are shown in Fig. 2b-d. LGA is formed during cellulose depolymerization via glycosidic cleavage followed by cyclic bridging at C1 and C6. Other than being used in the pharmaceutical industry, LGA can also be converted to various valuable chemicals, such as levoglucosenone, 5-hydroxymethylfurfural, styrene, and many more [45-48]. FF is produced from the dehydration of the cellulose chain or LGA. FF is a precursor and a key intermediate for producing a range of furan-based chemicals and solvents, such as furan, THF, lactic acid, levulinic acid, and furoic acid [49-51]. AGF is an isomer of LGA. When cellulose was converted alone, only 4.7% of LGA, 0.4% of AGF, and 0.4% of FF were produced after 25 min. Co-converting cellulose with equivalent PE, PP, or PS slightly lowered the monomer yields. PE, PP, and PS are thermally much more stable than cellulose. Plastic-derivable hydrocarbon compounds were not observed in post-reaction liquids, implying these plastic polymers did not

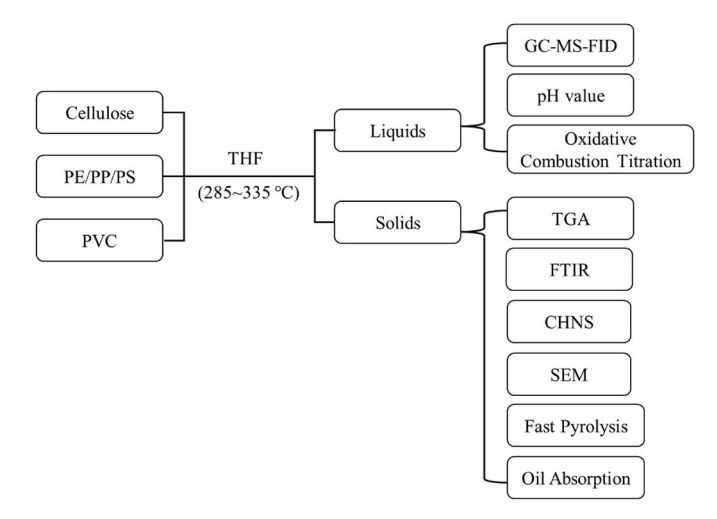


Fig. 1. Summary of experimental procedure.

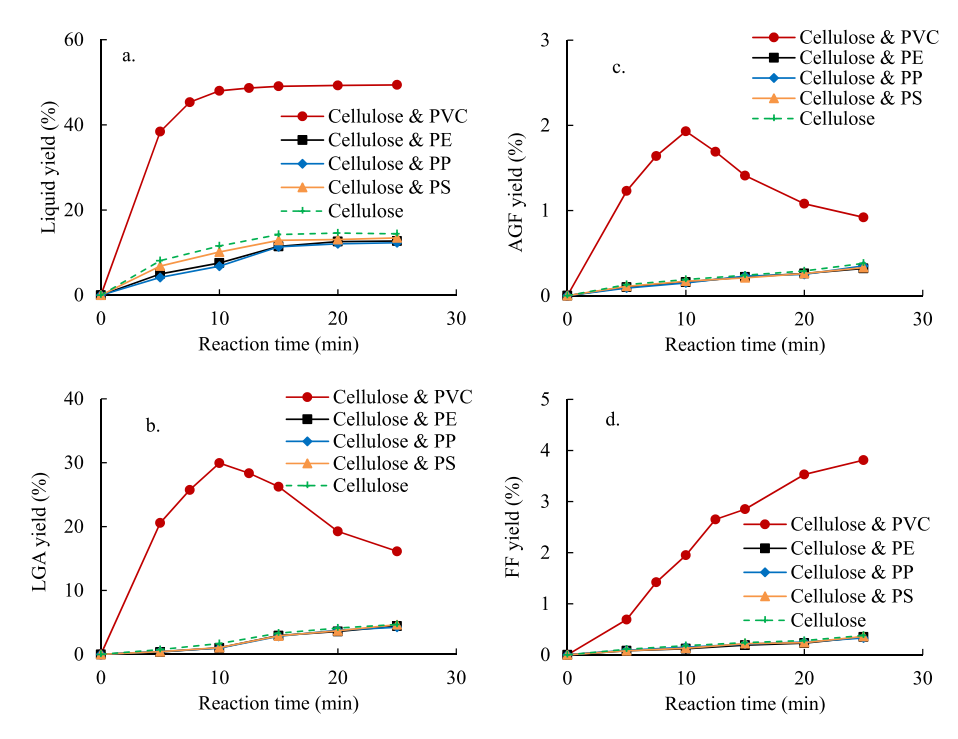


Fig. 2. Co-conversion of cellulose with different types of plastics in 310 °C THF (8:1 mass ratio of cellulose to PVC, 1:1 mass ratios of cellulose to other plastics). a. Liquid yield; b. LGA yield; c. AGF yield; d. FF yield. The "calculated" liquid yields were reported for cellulose or cellulose & PVC, the same applied to the rest of this article.

decompose during their co-conversion with cellulose in THF. The slightly decreased monomer yields and the liquid yields could be due to the heat and mass transfer limitations caused by the higher feedstock masses in the solvent. In comparison, an LGA yield of 30%, AGF yield of 1.9% (after 10 min), and FF yield of 3.8% (after 25 min) were achieved by co-converting cellulose with a small amount of PVC. Depolymerization and dehydration reactions of cellulose were strongly enhanced by co-converting cellulose and PVC, which are attributed to PVC-derived HCl in the solvent that serves acid catalyst [38]. During their co-conversion, PVC dehydrochlorination proceeded ahead of cellulose depolymerization to release HCl. Subsequently, the in-situ generated HCl catalyzed cellulose conversion in the solvent. In THF, cellulose is depolymerized into LGA and AGF since hydrolysis is not promoted in polar aprotic solvents. FF can be directly produced from the cellulose chain or when LGA or AGF further dehydrates [41,52]. The acid in the solvent can catalyze both cellulose depolymerization and dehydration [39,53]. LGA and AGF yields decreased with increasing reaction time after their optimal yields were reached due to secondary reactions to FF or others. Due to the enhanced dehydration, FF yield monotonically

Polyene

Polyene

Polyene

Howard and the control of the control o

Fig. 3. PVC-assisted cellulose depolymerization in polar aprotic solvent.

increased with increasing reaction time. The mechanism of the PVC-assisted cellulose conversion is illustrated in Fig. 3. Dehydrochlorination of PVC also produced polyene and was utilized in forming solid products in this work, which will be discussed later in this article.

3.2. Conversion of mixtures containing cellulose, PVC, and other hydrocarbon plastics

The above results show that cellulose and the hydrocarbon plastics (i. e., PE, PP, or PS) rarely interacted with their co-conversion, whereas co-conversion of cellulose and PVC strongly affected cellulose liquefaction to useful monomers. In the following sections, mixtures containing cellulose, PVC, and hydrocarbon plastics were converted to investigate how the presence of the hydrocarbon plastics affects the co-conversion reactions of cellulose and PVC, as well as recovered products.

3.2.1. Co-conversion using different solvent temperature

Mixtures of cellulose, PVC (8:1 ratio of cellulose to PVC), and cellulose equivalent mass of PE, PP, or PS were converted at 285, 310, and 335 °C. The results are given in Fig. 4. As shown in Fig. 4a, liquid yield increased with increasing reaction temperature for all the mixtures. In the case of cellulose, PVC, and PS, the optimum liquid yield was 49.1% at 285 °C, 50.9% at 310 °C, and 53.4% at 335 °C, respectively, achieved after 50 min, 15 min, and 10 min. When the "calculated" yield and actual yields were compared, it showed that the liquid yield slightly increased by adding PS to the mixture of cellulose and PVC, while it was reduced by adding PE or PP.

The liquid compositions did not vary by co-converting cellulose and PVC in the presence of hydrocarbon plastics. PE, PP, and PS-derivable compounds were not detected in any solvents. As shown in Fig. 4b–d, increasing reaction temperature significantly accelerated LGA, AGF, and FF formations and shortened the optimal reaction time. Higher solvent temperature promotes PVC dehydrochlorination, releasing HCl at a higher rate and readily catalyzing cellulose conversion. However, increasing solvent temperature also caused increased thermal degradations of LGA and AGF in the solvent containing the acid. Overall, 310 $^{\circ}\mathrm{C}$

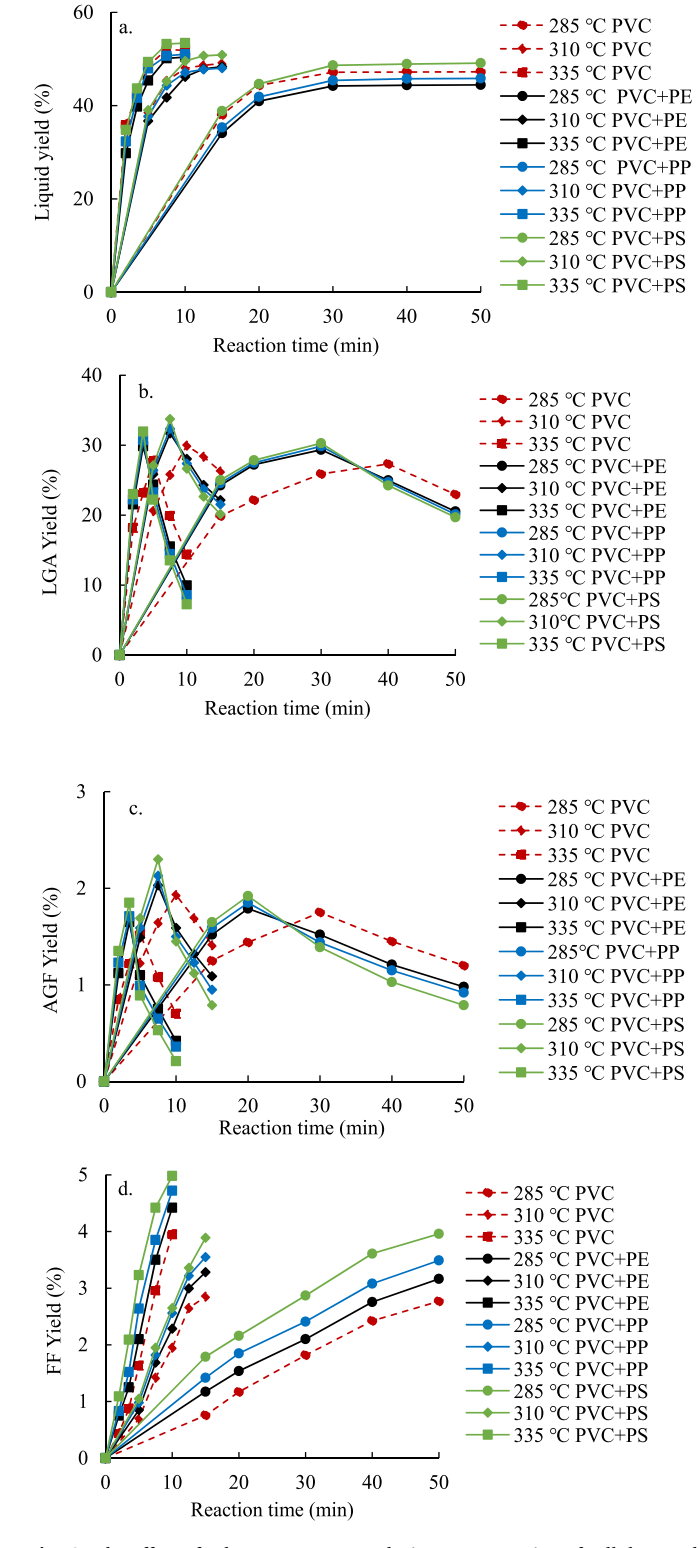


Fig. 4. The effect of solvent temperature during co-conversion of cellulose and varied plastics in THF (8:1 mass ratio of cellulose to PVC and 1:1 mass ratio of cellulose to PE, PP, or PS). a. Liquid yield; b. LGA yield; c. AGF yield; d. FF yield, as a function of reaction time.

was the optimal temperature for producing the highest LGA and AGF yields for all the cases. Since dehydration is promoted, FF yield increases with increasing solvent temperature and reaction time.

Surprisingly, PE, PP, or PS in their mixture with cellulose and PVC led to higher yields of LGA, AGF, and FF than co-converting cellulose

and PVC at all three different solvent temperatures. Adding PS had the most significant effect on promoting the monomer yields, followed by adding PP and PE. The optimum yields of LGA obtained at 310 $^{\circ}\text{C}$ and 7.5 min were 33.8%, 32.4%, and 31.7% for adding PS, PP, and PE, respectively. In comparison, the optimum LGA yield was 30% obtained after 10 min when cellulose and PVC were co-converted at the same temperature without other plastics. The promoting effect was also observed for FF as the highest FF yield of 5% was obtained after a 10 min reaction at 335 $^{\circ}\text{C}$ when adding PS. It also shows that the thermal stability of LGA and AGF decreased slightly by adding other plastics in the decreasing order of PE, PP, and PS, which will be discussed in section 3.2.3.

3.2.2. Co-conversion using different PVC loading

The effect of PVC loading in the feedstock was also investigated. In the feedstock mixtures, a constant mass ratio of 1:1 was used for cellulose to PE, PP, or PS, and varying mass ratios of 16:1, 8:1, and 4:1 were used for cellulose to PVC. In terms of choosing the mass ratios of cellulose, PVC, and PE, PP, or PS in the mixtures, smaller amounts of PVC than other compositions were used since PVC content in the real-world co-mingled MSW is usually much lower than other compositions [11,42, 54,55]. The solvent temperature of 310 °C was used in all cases. The results are given in Fig. 5. As shown in Fig. 5a, increasing PVC loading accelerated reactions to produce higher liquid yields. For cellulose, PVC, and PS mixtures, the maximum liquid yields were 44.2%, 49.8%, and 55.7% for cellulose to PVC mass ratios of 16:1, 8:1, and 4:1, obtained after 25 min, 15 min, and 12.5 min, respectively. Since higher PVC loading corresponds to a higher acid concentration in the reaction solvent, cellulose liquefaction was enhanced with increasing PVC loading in the feedstock. The liquid yields obtained from co-converting cellulose, PVC, and other plastics were comparable to or slightly lower than those of converting cellulose and PVC without other plastics. For the different PVC loadings, the highest liquid yields were always observed for converting the cellulose, PVC, and PS mixture, followed by the cellulose, PVC, and PP mixture, and finally, the cellulose, PVC, and PE mixture.

In Fig. 5b-d, the monomer yields in the liquids increased with increasing PVC loading due to the enhanced cellulose depolymerization and dehydration with higher solvent acidity. In the case of co-converting cellulose, PVC, and PS, the optimum yield of LGA increased from 31.9% to 33.8% and 35.4% by increasing the cellulose to PVC ratio from 16:1 to 8:1 and 4:1, respectively. For all three different PVC loadings, the presence of other plastics led to higher reaction rates and produced higher optimal monomer yields. As discussed, PS in the feedstock mixture promoted the most monomer yields, followed by PP and PE. For example, with a cellulose and PVC mass ratio of 4:1, the maximum LGA yields of 32.9%, 34.0%, and 35.4% were obtained after 5 min when PE, PP, and PS were presented, compared to the 30.7% obtained after 7.5 min without these plastics. Meanwhile, FF yield also increased from 4.1% to 4.4%, 4.7%, and 5.3% by adding PE, PP, or PS after 10 min. The effect of other plastics on increasing the monomer yields was slightly more noticeable when a higher PVC loading was used. It was also found that other plastics in the mixed feedstock increased the thermal instability of LGA and AGF in the order of PE, PP, and PS.

3.2.3. Chlorine distribution

As described above, although PE, PP, or PS nearly did not influence cellulose conversion when PVC was absent, they strongly affected the conversion when PVC was also present in their mixtures by promoting higher yields of cellulose-derived monomers and increasing reaction rates. Because PVC-derived HCl dissolved in THF acted as an acid catalyst, other plastics may have affected HCl concentration in the reaction solvent. Since HCl is *in-situ* generated, its concentration in the reaction solvent changes as PVC dehydrochlorination proceeds. On the other hand, CB (i.e., an organic chloride compound) was also formed whenever the feedstock contained PVC. CB is a reaction product between THF and HCl. Accordingly, the presence of CB proves the

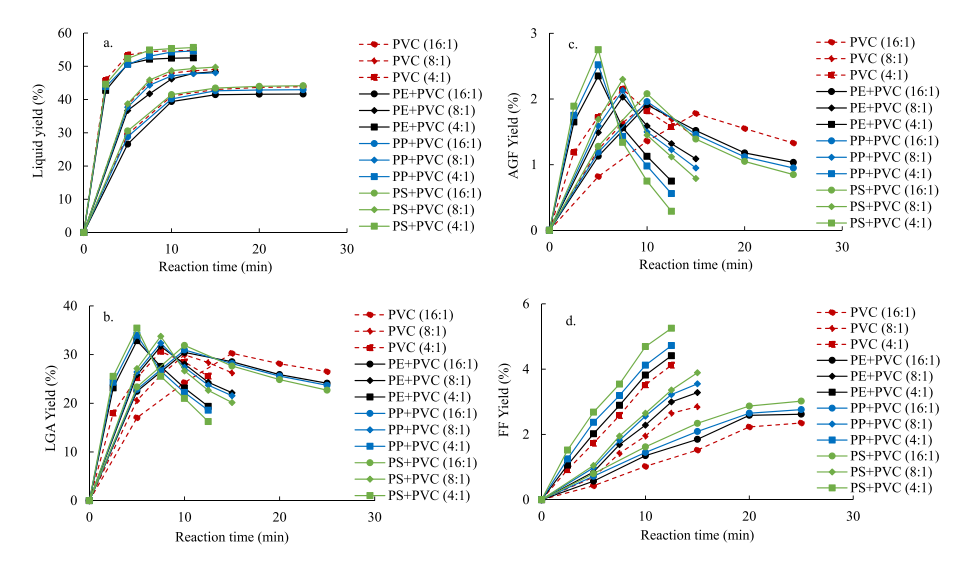


Fig. 5. The effect of PVC loading during co-conversion of cellulose and PVC with other plastics in 310 °C THF. a. Liquid yield; b. LGA yield; c. AGF yield, and d. FF yield.

secondary reaction of PVC-derived HCl in THF. Since CB formation consumes HCl, the acid concentration in the solvent during the conversion process is determined by the competing reactions between PVC dehydrochlorination (to HCl) and the secondary conversion of HCl (to CB). The time-resolved solvent acidity was investigated by measuring the solvent pH values at different reaction times with a reaction temperature of 310 °C. As shown in Fig. 6a, when PVC alone converted in THF, the solvent pH value decreased from 7 to 1.89 within the first 3.5 min due to the rapid dehydrochlorination of PVC. However, the pH value slightly increased at longer reaction times because of the secondary reaction of HCl, which is supported by the increased CB yield (per initial mass of PVC) along with increasing reaction time, as shown in Fig. 6b. Interestingly, the pH value decreased faster when PVC was converted when other plastics were also presented, resulting in a lower pH (i.e., a higher acidity) of the solvent. The lowest solvent pH was observed by adding PS compared to adding PP or PE. It was also found that CB yield became lower when other plastics were added, decreasing in the order of adding PE, PP, and PS. Therefore, the results imply that the secondary reaction of HCl to CB was suppressed when other plastics were presented, leading to higher acidity in the solvent. The solvent acidity was the strongest with PS because the conversion of HCl to CB was suppressed the most by PS. It is likely that due to the good solubility of PS in THF (compared to PE and PP that do not solubilize in THF) and its relatively lower thermal stability compared to PE and PP, some HCl was allured to decompose solubilized PS [56,57] instead of reacting with THF to produce CB. Since a higher solvent acidity accelerated cellulose conversion, higher monomer yields were obtained using shorter reaction times when other plastics were also presented. Meanwhile, higher acidity also caused LGA and AGF to become thermally less stable.

While HCl and CB were both derived from PVC, the fate of PVC-originated chlorine was also investigated by analyzing chlorine content in the solids based on the oxidative combustion titration method. Time-dependent chlorine distribution during the conversion of the PVC-containing mixtures is given in Fig. 6c. The content of inorganic chlorine (Cl⁻) was calculated by subtracting the contents of organic chlorine (i.e., Cl formed CB) and chlorine in the solids from the total chlorine content in PVC feedstock. The chlorine content in the solid decreased to 49% of the chlorine in the original PVC after 2.5 min for converting cellulose and PVC, and 52.2%, 53.7%, and 53.3%, respectively, by adding PE, PP, or PS. Chlorine was no longer detected in any solids recovered at 3.5 min and longer reaction times based on the analytical method used in this work. Thus, it is inferred that PVC dehydrochlorination was completed within the first 3.5 min of the reactions, and all or nearly all chlorine was

transferred into the liquid phase. Due to the secondary reaction of HCl to CB, the inorganic chlorine content reached a maximum and then decreased at longer reaction times, consistent with the time-dependent solvent pH profile previously given in Fig. 6a. The highest overall inorganic content was obtained when adding PS, followed by PP and PE, which also match the respective solvent pH profiles.

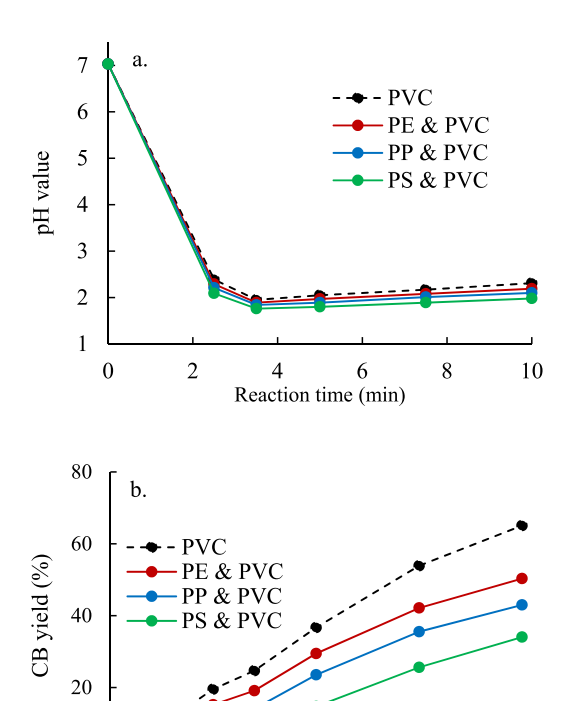
As shown above, chlorine in PVC was transformed to form HCl and CB in the liquid phase. CB is a functional monomer that can be used to analyze genotoxic impurities in active pharmaceutical ingredients. While CB can be extracted for chemical use, it can also be converted to THF and NaCl if NaOH is added to the post-reaction solvent. Adding NaOH can also convert inorganic chloride (HCl) to NaCl and $\rm H_2O$. These methods allow PVC chlorine to be recovered easily after the reactions without causing secondary pollution.

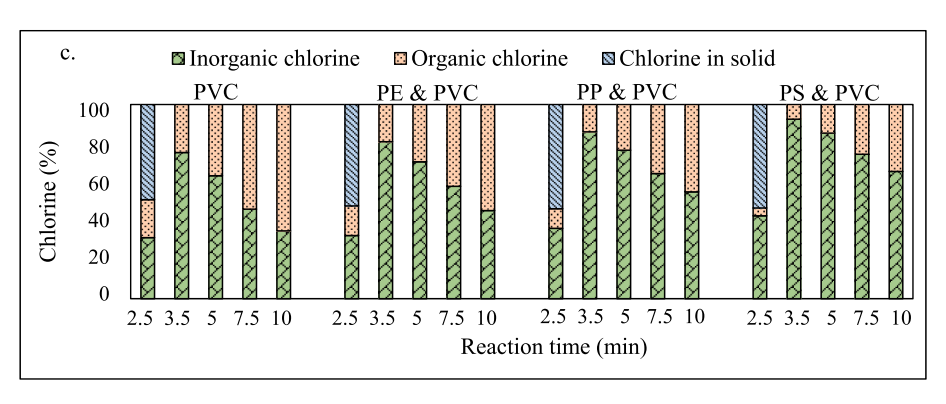
3.3. Characterization of solid products and their potential applications

3.3.1. TGA analysis results

The solids recovered in the reaction conditions that would produce the optimal LGA yields were analyzed for different feedstock compositions. The TGA and DTG results of the solids are compared with those of cellulose and plastics in Fig. 7.

In Fig. 7a, the TGA-based thermal decomposition of cellulose started at 260 °C and was completed by 400 °C, leaving 13.6% char. The three DTG peaks correspond to three stages of PVC decomposition (Fig. 7b). The first stage is due to the release of HCl. It is followed by the second stage associated with the continuing release of HCl and the release of benzene and other aromatic hydrocarbons. The third stage is due to the devolatilization of alkylbenzene and polyaromatic hydrocarbons [58]. There was 8.7% char remaining after PVC decomposition. Thermal decomposition of PE, PP, and PS started at higher temperatures than cellulose or PVC due to their higher thermal stability. No char was formed from either of them. During the TGA analysis, the solid products recovered from the mixed feedstock conversion in THF showed higher thermal stability than cellulose and PVC. For example, the solid recovered from the cellulose, PVC, and PE mixture conversion started to devolatilize at 380 °C, leaving 7% char. As shown in Fig. 7b, a single DTG peak appeared for all the solids. The DTG peak of PVC corresponding to HCl release was absent in the solids since PVC had been completely dechlorinated in THF when they were produced. The DTG peak temperature of the solids produced from the cellulose, PVC, PE mixture or the cellulose, PVC, and PP mixture was slightly lower than that of neat PE or PP. In comparison, the DTG peak temperature was





5 5 7 Reaction time (min)

7.5

10

0

Fig. 6. The results of time-resolved chlorine analysis during co-conversion of cellulose, PVC, and other plastics (a 4:1 mass ratio of cellulose and PVC; 310 °C). a. Solvent pH value; b. CB yield; c. Chlorine distribution.

slightly higher for the solid recovered from the cellulose, PVC, and PS mixture than neat PS. In all the solids, their DTG peak temperatures always occurred in the temperature regions between the third DTG peak of PVC (i.e., the peak corresponding to the devolatilization of dechlorinated PVC hydrocarbons) and the DTG peaks of the corresponding, neat non-PVC plastics. Thus, the shift in the DTG peaks of the solids could be attributed to the PVC-derived polyaromatic hydrocarbon residues present in the solids.

3.3.2. FTIR analysis results

FTIR spectra of the solids are given in Fig. 8. The spectra of neat cellulose, PVC, PE, PP, and PS are also included as references. For cellulose, the bands at $3000\text{-}3650~\mathrm{cm}^{-1}$ and $970\text{-}1080~\mathrm{cm}^{-1}$ are associated with O–H stretching and C–O stretching, respectively.

For PVC, the bands at 606 and 670 $\rm cm^{-1}$ are associated with C–Cl stretching in -CHCl groups. The bands at 2911 and 2955 $\rm cm^{-1}$ originate from aliphatic C–H. The band at 1424 $\rm cm^{-1}$ is due to C–H in CH₂, and the

band at 1236 cm⁻¹ is for C–H bending at -CHCl. In addition, the band at 953 cm⁻¹ is for C–H wagging [59,60]. In the solids, the cellulose-derived functional groups mostly disappeared, and the Cl-associated bands of PVC were also nearly eliminated. While the FTIR spectrum of the solids was largely similar to that of the corresponding hydrocarbon plastics in the feedstock mixtures from which the solids were derived, there were also some differences. For example, the bands for O–H and C–O related to cellulose presented in low intensities. Additionally, the aromatic ring band (1500 cm⁻¹) either newly appeared or emphasized in the solids, attributed to cellulose-derived char and PVC-derived polyaromatics. The polyenes formed during PVC dechlorination reactions are highly reactive and further aromatize to form polyaromatics. Therefore, the FTIR spectra confirm that the hydrocarbon plastics, cellulose-derived char, and PVC-derived aromatic hydrocarbons all contributed to the solid structures

Compared to their corresponding neat plastics, small peaks of C=C at $1600-1670~{\rm cm}^{-1}$ newly appeared in the FTIRs of the solids caused by

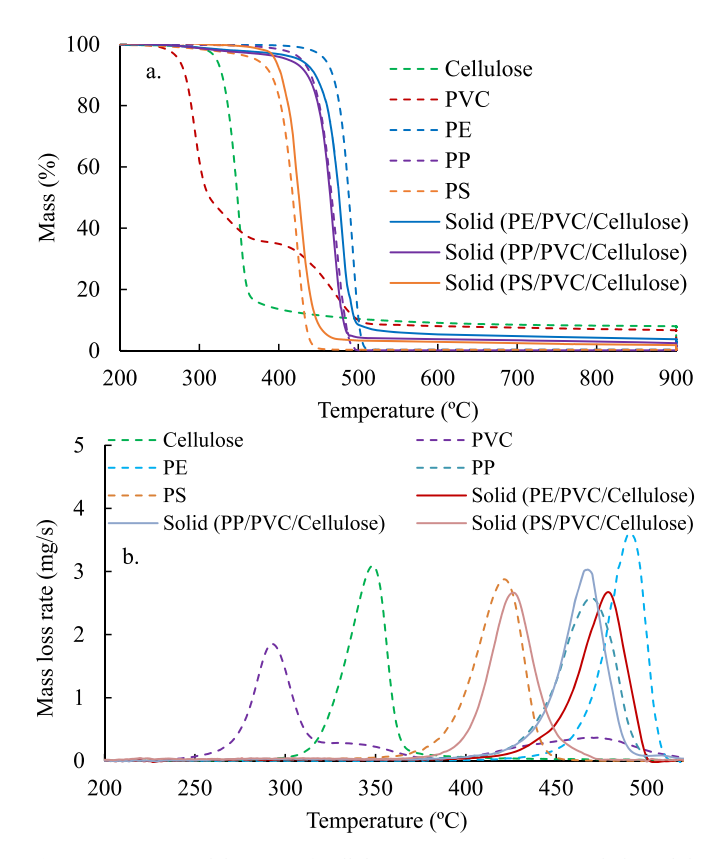


Fig. 7. A. TGA, and b. DTG of cellulose, PVC, PE, PP, PS, and the solids recovered from the conversion of their mixtures. The reaction conditions for producing the solids are 310 $^{\circ}$ C THF, 7.5 min, and a 4:1 mass ratio of cellulose to PVC.

the slight fragmentations of the hydrocarbon chains of these plastics during the co-conversion in THF. The unstable C=C likely crosslinked with highly reactive PVC-originated polyenes to form structures different than the original plastics, confirmed by the TGA results. In addition, the TGA results showed that the thermal stability of the plastics decreased in the order of PE, PP, and PS. PS has lower thermal stability than PE or PP, which explains the highest peak of C=C on FTIR spectra for the PS-containing mixture-derived solid, followed by the PPcontaining mixture-derived solid and the PE-containing mixture-derived solid. Although the solvent temperatures in this study (up to 335 $^{\circ}$ C) were lower than the thermal decomposition temperatures of PE, PP, or PS, the solvent's acidity due to PVC-derived HCl can promote their chain fragmentations at lower temperatures. The more reactive the plastic, the more hydrogen ions will have the propensity to participate in plastic depolymerization and thus lead to more C=C on the chain. Since HCl was also used to catalyze plastic depolymerization, its chance for the secondary reaction with THF was reduced. On the other hand, hydrogen atoms can be released from the plastics during their chain cleavages, increasing the hydrogen content in the solvent to affect the solvent acidity. The solvent acidity affected by the presence of PE, PP, or PS further affected the conversion rate and the monomer yields described above.

3.3.3. Pyrolysis of the solid products

The compositions of the solids were further investigated by fast pyrolyzing the solids and analyzing the vapors. In their GC/MS chromatograms (Fig. S1), chlorine-related compounds were not detected among the pyrolysis vapors of the solids, confirming the effective dechlorination by solvent-based conversion. Pyrolysis of the solids produced diverse hydrocarbon products similar to pyrolyzing the corresponding neat hydrocarbon plastics, However, the selectivity of

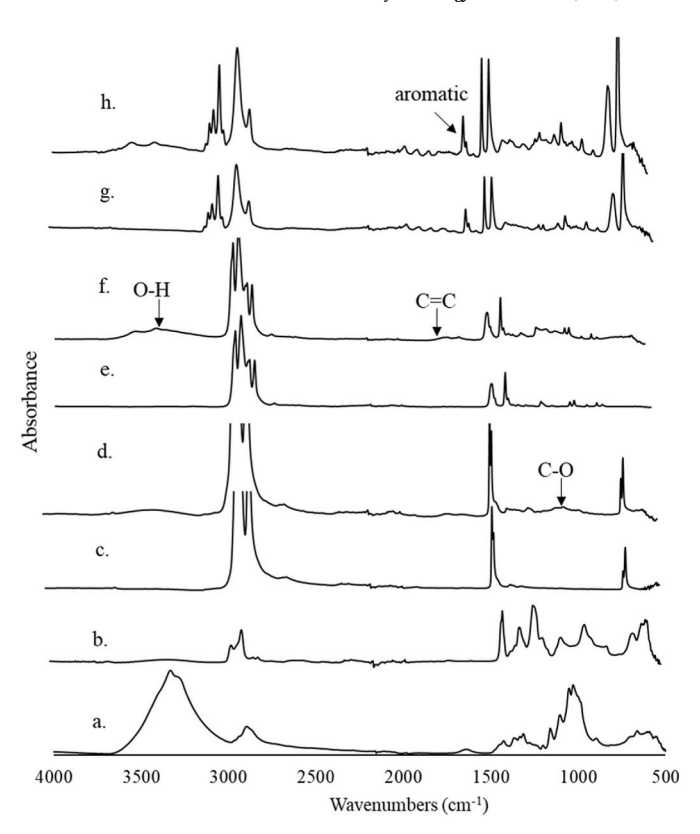


Fig. 8. FTIR spectra of cellulose, untreated plastics, and the solids recovered during co-conversion of cellulose, PVC, and other plastics with a 4:1 ratio of cellulose to PVC in 310 °C THF. a. Cellulose; b. PVC; c. PE; d. Solid recovered from the conversion of PE-containing mixture at 7.5 min; e. PP; f. Solid recovered from the conversion of PP-containing mixture at 7.5 min; g. PS; h. Solid recovered from the conversion of the PS-containing mixture at 7.5 min.

individual compounds among the pyrolysis products was different. When the same amounts of samples were pyrolyzed, the solid recovered from the cellulose, PVC, and PE mixture produced similar peak intenstites of long-chain hydrocarbons (C20-C30) but slightly higher intensities of medium-chain hydrocarbons (C10-C20) and slightly lower intensities of short-chain hydrocarbons (C5-C10) than neat PE. It also shows that pyrolyzing the solid recovered from the cellulose, PVC, and PP mixture produced higher amounts of the GC/MS-detectable aliphatic hydrocarbons (i.e., relatively lower molecular weight compounds) than pure PP. While aromatics, such as toluene and styrene, were the major pyrolysis products of both PS and the solid recovered from the cellulose, PVC, and PS mixture, the product selectivity was also slightly different. For instance, compared to neat PS, the solid produced a larger amount of toluene and styrene but less methyl styrene. The above results show that the solids recovered after the co-conversions are no longer intact hydrocarbon plastics. On the other hand, the pyrolysis results also suggest that the solids could be depolymerized to produce liquid hydrocarbon fuels and chemicals.

3.3.4. Elemental analysis results

Elemental compositions and HHVs of the solids are given in Table S1. There were 4.21%, 3.28%, and 3.09% oxygen in the solids recovered from the cellulose and PVC mixed with PE, PP, or PS. The small percentages of oxygen in the solids are attributed to cellulose-derived chars.

As described above, adding the hydrocarbon plastics increased the solvent acidity in the order of PE < PP < PS. Since the oxygen content of solids was in the reverse order, the results suggest that the higher solvent acidity promoted the deoxygenation of the cellulose-derived char. The HHV of the solid recovered from the cellulose, PVC, and PP mixture was 46.11 MJ/kg, higher than 45.03 MJ/kg for the solid recovered from the

cellulose, PVC, and PE mixture. Despite its lowest oxygen content, the solid recovered from the cellulose, PVC, and PS mixture had the lowest HHV of 40.13 MJ/kg due to the lower hydrogen content in PS than in PE or PP. The high HHVs of the solids were contributed by the hydrocarbon plastics and the PVC-derived polyaromatics remaining in the solids. It is highly possible that there dechlorinated PVC reacted with the hydrocarbon plastics in the solids. Since chlorine was removed during the conversion in THF, the solids could also be used as clean, high-quality fuels. In the PVC-assisted conversions demonstrated in this study, while PVC-derived HCl is utilized in the liquid to catalyze chemical formations and produce recoverable Cl products, the hydrocarbons of PVC molecules could also be recycled as high-quality solid fuels.

3.3.5. SEM results

The microstructures of the solids are given in Fig. 9. Other than the SEM images of the solids recovered from converting the mixtures of cellulose and PVC with the hydrocarbon plastics in THF, neat PE, PP, PS, and the solids recovered from converting the mixtures of PVC with PE, PP, or PS in THF without cellulose were also included to evaluate the effect of cellulose feedstock on the solid morphology. Additionally,

hydrothermal chars prepared by converting the mixtures of cellulose, PVC, and other plastics in water were also analyzed to determine the solvent effect. Their SEM images were also included in determining the effect of using THF as the solvent.

Compared to the neat PE particles in Fig. 9a, a slightly flaked solid was observed when PE was co-converted with PVC in THF (Fig. 9d). On the other hand, the solid recovered from the cellulose, PVC, and PE mixture in THF had a significantly different microstructure (Fig. 9g), where nanoscale particles are attached to wrinkled microfilaments to create a large surface area. Such a microstructure of the solid was also completely different than the hydrothermal char produced using the same feedstock. As shown in Fig. 9j, the hydrothermal char had a dense structure with some shallow pores on the surface.

In the case of PP, the solid recovered from the co-conversion of PVC and PP in THF had a sponge-like structure of microparticles (Fig. 9e) compared to the dense structure of neat PP (Fig. 9b). On the other hand, a porous sponge-like structure containing microfilaments was observed for the solid recovered from the cellulose, PVC, and PP mixture in THF (Fig. 9h). The hydrothermal char produced using the same feedstock had a smooth surface with hollow and large pores (Fig. 9k).

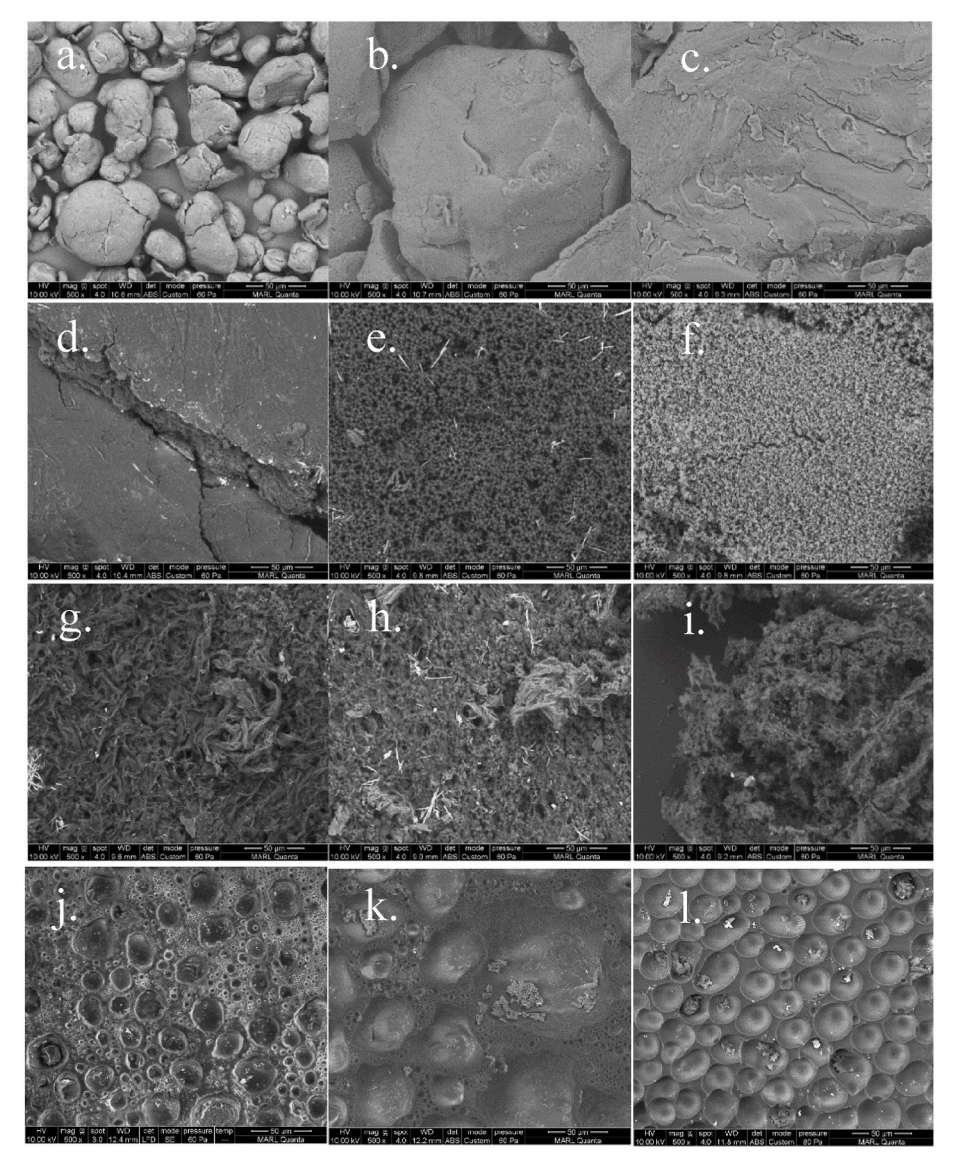


Fig. 9. SEM results. a-c. Neat PE, PP, and PS; d-f. The solids recovered when PVC was co-converted with PE, PP, or PS in THF; g-i. The solids recovered when cellulose and PVC were co-converted with PE, PP, or PS in THF; j-l. The hydrothermal chars recovered when cellulose and PVC were co-converted with PE, PP, or PS in water. The reaction conditions for producing the solids are 310 °C, 7.5 min, and a 4:1 mass ratio of cellulose to PVC.

In the case of PS, neat PS had a dense and continuous structure (Fig. 9c), whereas the solid recovered from the co-conversion of PS and PVC in THF showed agglomerated sphere microparticles (Fig. 9f). In comparison, the solid recovered from the cellulose, PVC, and PS mixture in THF had a sponge-like structure where microfilaments and nanospheres were agglomerated (Fig. 9i). The hydrothermal char derived from the PS-containing mixture was similar to other hydrothermal chars described above, mostly molten plastics (Fig. 91). These results demonstrate that the solid morphologies relate to feedstock compositions and the conversion solvent. It is speculated that cellulose-derived carbonized char, dechlorinated PVC polyenes, and non-PVC plastics physically and chemically interacted to form the solids with unique microstructures. Other than feedstock compositions, the reaction solvent also played an important role. As described in the introduction, water is a polar protic solvent, whereas THF is a polar aprotic solvent. Thus, cellulose does not hydrolyze in THF. On the other hand, the catalytic effect of HCl can be greatly magnified in THF, which can reduce the activation energy of cellulose decomposition [61]. While it requires further investigation, using THF as the solvent may also improve the compatibility of different feedstock compositions in the solvent to affect their interactions.

3.3.6. Solids as oil absorbents

The chemical properties and morphology of the solids described above suggest that the solids may also be used as oil absorbents. Due to the increasing maritime activities and oil exploration, oil spills are happening daily, which has caused a wide range of short-term and long-term damage to the ecosystems and human health [62,63]. Therefore, cleaning and recovering spilled oils have been urgent but challenging. Materials with a porous structure have shown the potential to separate the oil from the ocean water because of good absorption capacity and efficiency [64–67]. The solids recovered from the cellulose, PVC, and other plastic mixtures in THF had three-dimensional porous structures and exhibited hydrophobicity resulting from the plastic-derived hydrocarbons [44]. These characteristics of the solids are attractive to their potential application as oil absorbents.

The oil absorption capacity of the solids was preliminarily investigated by conducting water-oil separation experiments using paraffin oil and canola oil. As a comparison, the absorbent experiments were also conducted using the hydrothermal chars derived from the same feedstock compositions. As shown in Fig. S2, the solids could effectively absorb the oils from water. The results of the absorption capacity of the solids for absorbing the two types of oils were compared to that of hydrothermal chars in Fig. 10. Overall, the solids recovered using THF as the conversion solvent constantly outperformed the hydrothermal chars. Among the solids, the solid recovered from the cellulose, PVC, and PE mixture had the highest absorption capacity, followed by the solids recovered from the cellulose and PVC with PP and the cellulose and PVC mixed with PS. Furthermore, the absorption capacities of the solids did not vary significantly by using the two different types of oils. For example, the absorption capacity of the solid recovered from the cellulose, PVC, and PE mixture in THF was 360% and 357% for paraffin oil and canola oil, respectively, compared to 17% and 15% for the hydrothermal char recovered using the same feedstock composition but using water as the solvent. The good properties of oil absorbents require qualities such as good mutual solubility, high surface area, porous structure, penetration into a network structure, and a low degree of crosslinking [44]. The solids either had a structure with wrinkled microfilaments that could provide a high surface area or sponge-like penetrative structures. Among the solids, the solid derived from the cellulose, PVC, and PE mixture also has linear hydrocarbons with some small amounts of oxygenated groups (as shown in FTIR and elemental analysis results), providing a chemically compatible structure to the oils. PE also had higher thermal stability than PP and PS, which led to the least crosslinking in the PE-based solid, as confirmed by TGA and FTIR results.

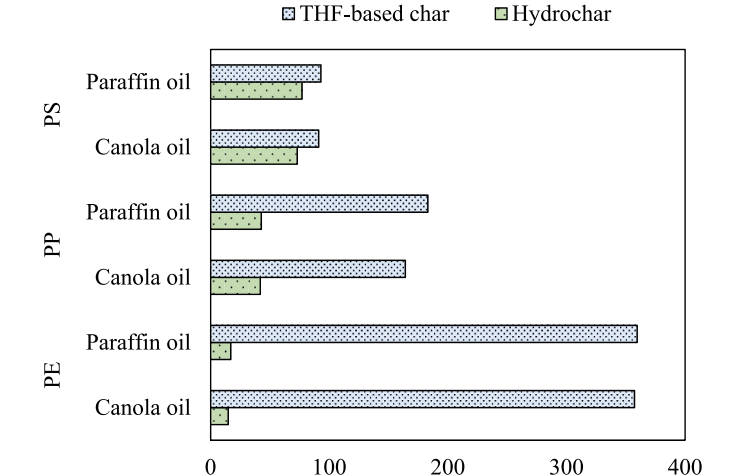


Fig. 10. The oil absorption capacity of solids compared to hydrothermal chars for absorbing two types of oils. The solids and hydrothermal chars were recovered when cellulose and PVC were co-converted with PE, PP, or PS, respectively, in 310 $^{\circ}$ C THF or water at 7.5 min (a 4:1 mass ratio of cellulose to PVC).

Absorption capacity (%)

3.4. Conclusions

A single-step upcycling of PVC-containing commingled solid wastes in THF was demonstrated using cellulose, PVC, PE, PP, and PS as the model compositions. When co-converted, cellulose was selectively converted to up to 35.4% LGA and 5.3% FF due to the catalytic effects of PVC-released HCl and the effect of non-PVC plastics on suppressing the secondary reaction of HCl. During the conversions in THF, PVC chlorine staved in the liquid as chloride ions or CB, can be recovered easily. The dechlorinated solid products had an HHV of up to 46.11 MJ/kg; thus. they can be used as clean, high-quality fuels or pyrolyzed to produce hydrocarbon compounds. These solids also showed excellent oilabsorbing capability. Overall, the present work provides a promising approach to recycling PVC-containing mixture wastes into multiple value-added products by leveraging the intrinsic properties of different waste feedstock compositions. While the model mixtures were used in this study to mimic MSW, the effect of the impurities present in real wastes, such as dyes and other minor polymers will be determined in future work. Additionally, technoeconomic analysis will evaluate the economic viability of this pathway, compare different feedstock scenarios, and identify key contributors to product costs.

Declaration of competing interest

No competing interest to report.

Acknowledgment

The research is supported by the National Science Foundation (grants No. 1803823 & 1826978).

Appendix A. Supplementary data

Supplementary data to this article can be found online at https://doi.org/10.1016/j.joei.2023.101405.

References

PlascticsEurope, Plastics - the Facts 2020, 2020. https://plasticseurope.org/wp-content/uploads/2021/09/Plastics_the_facts-WEB-2020_versionJun21_final.pdf.

- [2] L. Lebreton, A. Andrady, Future scenarios of global plastic waste generation and disposal, Palgrave Commun. 5 (2019), https://doi.org/10.1057/s41599-018-0212-
- [3] B. Bai, H. Jin, C. Fan, C. Cao, W. Wei, W. Cao, Experimental investigation on liquefaction of plastic waste to oil in Supercritical Water, Waste Manag. 89 (2019) 247-253, https://doi.org/10.1016/j.wasman.2019.04.017.
- [4] B.C. Gibb, Plastics are forever, Nat. Chem. 11 (2019) 394–395, https://doi.org/ 10.1038/s41557-019-0260-7
- [5] F. Zhang, Y. Zhao, D. Wang, M. Yan, J. Zhang, P. Zhang, T. Ding, L. Chen, C. Chen, Current technologies for plastic waste treatment: a review, J. Clean. Prod. 282 doi.org/10.1016/j.jclepro.2020.1245
- [6] R. Geyer, J.R. Jambeck, K.L. Law, Production, use, and fate of all plastics ever made, Sci. Adv. 3 (2017), https://doi.org/10.1126/sciadv.1700782
- [7] J.M. Garcia, M.L. Robertson, The future of plastics recycling, Science 358 (2017) 870-872, https://doi.org/10.1126/science.aaq032
- [8] S. Colantonio, L. Cafiero, D. De Angelis, N.M. Ippolito, R. Tuffi, S.V. Ciprioti, Thermal and catalytic pyrolysis of a synthetic mixture representative of packaging plastics residue, Front. Chem. Sci. Eng. 14 (2019) 288-303, https://doi.org/
- [9] E.L. Teuten, J.M. Saquing, D.R. Knappe, M.A. Barlaz, S. Jonsson, A. Björn, S. J. Rowland, R.C. Thompson, T.S. Galloway, R. Yamashita, D. Ochi, Y. Watanuki, C. Moore, P.H. Viet, T.S. Tana, M. Prudente, R. Boonyatumanond, M.P. Zakaria, K. Akkhavong, Y. Ogata, H. Hirai, S. Iwasa, K. Mizukawa, Y. Hagino, A. Imamura, M. Saha, H. Takada, Transport and release of chemicals from plastics to the environment and to Wildlife, Phil. Trans. Biol. Sci. 364 (2009) 2027-2045, https:// doi.org/10.1098/rstb.2008.0284.
- [10] R. Verma, K.S. Vinoda, M. Papireddy, A.N.S. Gowda, Toxic pollutants from plastic waste- A Review, Proc. Environ. Sci. 35 (2016) 701-708, https://doi.org/10.1016/ proeny 2016 07 069
- [11] EPA, Plastics: Material-specific Data, 2021. https://www.epa.gov/facts-and-figure bout-materials-waste-and-recycling/plastics-material-specific-data.
- [12] S. Watanabe, K. Kitamura, M. Nagahashi, Effects of dioxins on human health: a review, J. Epidemiol. 9 (1999) 1–13, https://doi.org/10.2188/jea.9.1.
- [13] M. Kogevinas, Human health effects of dioxins: cancer, reproductive and endocrine system effects, APMIS 109 (2001), https://doi.org/10.1111/j.1600-0463.2001
- [14] M. Sadat-Shojai, G.-R. Bakhshandeh, Recycling of PVC wastes, Polym. Degrad. Stabil. 96 (2011) 404-415, https://doi.org/10.1016/j. olymdegradstab.2010.12.001
- [15] K. Lewadiwski, K. Skórczewska, A brief review of poly(vinyl Chlroide) (PVC) Recycling, Polymers 14 (2022) 3035, https://doi.org/10.3390/polym14153035. L.M.F. Paolo, Recycling of PVC and Mixed Plastic Waste, ChemTec Publishing,
- [16] Γoronto, 1996.
- [17] D. Braun, Recycling of PVC, Prog. Polym. Sci. 27 (2002) 2171-2195, https://doi. z/10.1016/s0079-6700(02)00036-9
- [18] J. Yu, L. Sun, C. Ma, Y. Qiao, H. Yao, Thermal degradation of PVC: a review, Waste Manag. 48 (2016) 300-314, https://doi.org/10.1016/J.WASMAN.2015.11.041.
- [19] N. Sophonrat, L. Sandström, R. Svanberg, T. Han, S. Dvinskikh, C.M. Lousada, W. Yang, Ex situ catalytic pyrolysis of a mixture of polyvinyl chloride and cellulose using calcium oxide for HCl adsorption and catalytic reforming of the pyrolysis products, Ind. Eng. Chem. Res. 58 (31) (2019) 13960–13970, https://doi.org/ 10.1021/acs.jecr.9b02299.
- [20] Y.m Matsuzawa, M. Ayabe, J. Nishino, Acceleration of Cellulose Co-pyrolysis with Polymer Polymer Degradation and Stability, vol. 71, 2001, pp. 435-444, https:// loi.org/10.1016/S0141-3910(00)00195-6, 3.
- [21] H. Zhou, C. Wu, J.A. Onwudili, A. Meng, Y. Zhang, P.T. Williams, Effect of interactions of PVC and biomass components on the formation of polycyclic aromatic hydrocarbons (PAH) during fast co-pyrolysis, RSC Adv. 5 (2015)
- 11371–11377, https://doi.org/10.1039/c4ra10639c. [22] H. Yu, J. Qu, Y. Liu, H. Yun, X. Li, C. Zhou, Y. Jin, C. Zhang, J. Dai, X. Bi, Copyrolysis of biomass and polyvinyl chloride under microwave irradiation, Distribution of chlorine Science of The Total Environment 806 (4) (2022), 150903, https://doi.org/10.1016/j.scitotenv.2021.150903.
- [23] Q. Huang, Y. Tang, S. Wang, Y. Chi, J. Yan, Effect of cellulose and polyvinyl chloride interactions on the catalytic cracking of tar contained in syngas, Energy Fuel. 30 (2016) 4888-4894, https://doi.org/10.1021/acs.energyfuels.6b00432
- [24] H. Kuramochi, D. Nakajima, S. Goto, K. Sugita, W. Wu, K. Kawamoto, HCl emission during co-pyrolysis of Demolition Wood with a small amount of PVC film and the effect of wood constituents on HCl emission reduction, Fuel 87 (2008) 3155-3157, s://doi.org/10.1016/j.fuel.2008.03.021
- [25] N. Miskolczi, L. Bartha, A. Angyal, Pyrolysis of polyvinyl chloride (PVC)-containing mixed plastic wastes for recovery of hydrocarbons, Energy Fuel. 23 (2009) 2743-2749, https://doi.org/10.1021/ef8011245
- [26] Z. Xu, J.W. Albrecht, S.S. Kolapkar, S. Zinchik, E. Bar-Ziv, Chlorine removal from U.S. solid waste blends through torrefaction, Appl. Sci. 10 (2020) 3337, https:// oi.org/10.3390/app10093337.
- [27] Y. Shen, A review on hydrothermal carbonization of biomass and plastic wastes to energy products, Biomass Bioenergy 134 (2020), 105479, https://doi.org/ 10.1016/j.biombioe.2020.105479
- [28] Q. Wang, S. Wu, D. Cui, H. Zhou, D. Wu, S. Pan, F. Xu, Z. Wang, Co-hydrothermal carbonization of organic solid wastes to Hydrochar as potential fuel: a Review, Sci. Total Environ. 850 (2022), 158034, https://doi.org/10.1016/j scitotenv.2022.158034.
- [29] Z. Yao, X. Ma, A new approach to transforming PVC waste into energy via combined hydrothermal carbonization and fast pyrolysis, Energy 141 (2017) 1156-1165, https://doi.org/10.1016/j.energy.2017.10.008.

- [30] D. Ma, L. Liang, E. Hu, H. Chen, D. Wang, C. He, Q. Feng, Dechlorination of polyvinyl chloride by hydrothermal treatment with Cupric Ion, Process Saf. Environ. Protect. 146 (2021) 108–117, https://doi.org/10.1016/ ep.2020.08.040.
- [31] Y. Wang, K. Wu, Q. Liu, H. Zhang, Low chlorine oil production through fast pyrolysis of mixed plastics combined with Hydrothermal Dechlorination Pretreatment, Process Saf. Environ. Protect. 149 (2021) 105–114, https://doi.org/ 10.1016/j.psep.2020.10.023
- [32] X. Lu, X. Ma, X. Chen, Z. Yao, C. Zhang, Co-hydrothermal carbonization of polyvinyl chloride and Corncob for Clean Solid Fuel production, Bioresour. Technol. 301 (2020), 122763, https://doi.org/10.1016/j.biortech.2020.122763.
- [33] C. Zhang, X. Ma, T. Huang, Y. Zhou, Y. Tian, Co-hydrothermal carbonization of Water Hyacinth and polyvinyl chloride: optimization of process parameters and characterization of Hydrochar, Bioresour. Technol. 314 (2020), 123676, https:// loi.org/10.1016/i.biortech.2020.123676
- [34] Z. Xu, R. Qi, D. Zhang, Y. Gao, M. Xiong, W. Chen, Co-hydrothermal carbonization of Cotton Textile Waste and polyvinyl chloride waste for the production of solid fuel: interaction Mechanisms and combustion behaviors, J. Clean. Prod. 316 (2021), 128306, https://doi.org/10.1016/j.jclepro.2021.1283
- [35] H.-Z. Li, Y.-N. Zhang, J.-Z. Guo, J.-Q. Lv, W.-W. Huan, B. Li, Preparation of hydrochar with high adsorption performance for methylene blue by cohydrothermal carbonization of polyvinyl chloride and Bamboo, Bioresour. Technol. 337 (2021), 125442, https://doi.org/10.1016/j.biortech.2021.125442.
- Y. Wei, S. Fakudze, Y. Zhang, R. Ma, Q. Shang, J. Chen, C. Liu, Q. Chu, Cohydrothermal carbonization of pomelo peel and PVC for production of hydrochar pellets with enhanced fuel properties and dechlorination, Energy 239 (2022), 122350, https://doi.org/10.1016/j.energy.2021.122350.
- [37] J. Braden, X. Bai, Production of biofuel precursor chemicals from the mixture of cellulose and polyvinylchloride in polar aprotic solvent, Waste Manag. 78 (2018) 894-902, https://doi.org/10.1016/j.wasman.2018.07.011.
- X. Chen, X. Bai, Co-conversion of wood and polyvinyl chloride to valuable chemicals and high-quality solid fuel, Waste Manag. 144 (2022) 376-386, https:// doi.org/10.1016/j.wasman.2022.04.018.
- [39] A. Ghosh, X. Bai, R.C. Brown, Solubilized carbohydrate production by acidcatalyzed depolymerization of cellulose in polar aprotic solvents, ChemistrySelect 3 (2018) 4777–4785, https://doi.org/10.1002/slct.201800764
- J.S. Luterbacher, J.M. Rand, D.M. Alonso, J. Han, J.T. Youngquist, C.T. Maravelias, B.F. Pfleger, J.A. Dumesic, Nonenzymatic sugar production from biomass using biomass-derived γ-Valerolactone, Science 343 (2014) 277–280, https://doi.org/ 10.1126/science.1246748.
- [41] A. Ghosh, R.C. Brown, X. Bai, Production of solubilized carbohydrate from cellulose using non-catalytic, supercritical depolymerization in polar aprotic solvents, Green Chem. 18 (2016) 1023-1031, https://doi.org/10.1039/ 5gc02071a
- [42] M. Biron, The plastics industry, Thermosets and Composites (2014) 25-104, https://doi.org/10.1016/b978-1-4557-3124-4.00002-x
- J. Long, Q. Zhang, T. Wang, X. Zhang, Y. Xu, L. Ma, An efficient and economical process for lignin depolymerization in biomass-derived solvent tetrahydrofuran, Bioresour. Technol. 154 (2014) 10–17, https://doi.org/10.1016/j. biortech 2013 12 020
- [44] J. Saleem, M. Adil Riaz, M.K. Gordon, Oil sorbents from plastic wastes and polymers: a Review, J. Hazard Mater. 341 (2018) 424-437, https://doi.org/ 0.1016/j.jhazmat.2017.07.072
- [45] M.A. Bergauff, T.J. Ward, C.W. Noonan, C.T. Migliaccio, C.D. Simpson, A. R. Evanoski, C.P. Palmer, Urinary Levoglucosan as a biomarker of wood smoke: results of human exposure studies, J. Expo. Sci. Environ. Epidemiol. 20 (2009) 385-392, https://doi.org/10.1038/jes.2009.46.
- F. Cao, T.J. Schwartz, D.J. McClelland, S.H. Krishna, J.A. Dumesic, G.W. Huber, Dehydration of cellulose to levoglucosenone using polar aprotic solvents, Energy Environ. Sci. 8 (2015) 1808-1815, https://doi.org/10.1039/c5ee0035
- J. He, M. Liu, K. Huang, T.W. Walker, C.T. Maravelias, J.A. Dumesic, G.W. Huber, Production of levoglucosenone and 5-hydroxymethylfurfural from cellulose in polar aprotic solvent-water mixtures, Green Chem. 19 (2017) 3642-3653, https:// doi.org/10.1039/c7gc01688c
- [48] I. Itabaiana Junior, M. Avelar do Nascimento, R.O. de Souza, A. Dufour, R. Wojcieszak, Levoglucosan: a promising platform molecule? Green Chem. 22 (2020) 5859-5880, https://doi.org/10.1039/d0gc01490g
- M. Kabbour, R. Luque, Furfural as a platform chemical. Biomass, Biofuels, Biochemicals (2020) 283-297, https://doi.org/10.1016/b978-0-444-64307-
- P. Khemthong, C. Yimsukanan, T. Narkkun, A. Srifa, T. Witoon, S. Pongchaiphol, S. Kiatphuengporn, K. Faungnawakij, Advances in catalytic production of value added biochemicals and biofuels via furfural platform derived lignocellulosic biomass, Biomass Bioenergy 148 (2021), 106033, https://doi.org/10.1016/j biombioe, 2021, 106033.
- [51] A. Jaswal, P.P. Singh, T. Mondal, Furfural a versatile, biomass-derived platform chemical for the production of Renewable Chemicals, Green Chem. 24 (2022) 510-551, https://doi.org/10.1039/d1gc0327
- X. Bai, R.C. Brown, J. Fu, B.H. Shanks, M. Kieffer, The influence of alkali and alkaline earth metals and the role of acid pretreatments in the production of sugars from switchgrass based on solvent liquefaction, Energy Fuel. 28 (2014) 1111-1120, https://doi.org/10.1021/ef4022015
- 4-Chloro-1-butanol, tech. 85%, Thermo Scientific | Fisher Scientific. https://www. fishersci.com/shop/products/4-chloro-1-butanol-tech-85-thermo-scientific/ AAL0404218#:~:text=4%2DChloro%2D1%2Dbutanol%20is%20employed%20as %20an%20internal,ingredients%20by%20GC%2DMS%20technique.&

- text = Soluble %20 in %20 methanol %2C%20 chloroform %2C%20 and %20 dimethyl %20 sufoxide.
- [54] N.C. Billingham, M. Bonora, D. de Corte, Environmentally degradable plastics based on oxo-biodegradation of conventional polyolefins, Biodegradable Polym. Plast. (2003) 313–325, https://doi.org/10.1007/978-1-4419-9240-6_21.
- [55] Y.V. Vazquez, F. Barragán, L.A. Castillo, S.E. Barbosa, Analysis of the relationship between the amount and type of MSW and population socioeconomic level: bahfa Blanca case study, Argentina, Heliyon 6 (2020), https://doi.org/10.1016/j. heliyon.2020.e04343.
- [56] V. Karmore, G. Madras, Thermal degradation of polystyrene by Lewis acids in solution, Ind. Eng. Chem. Res. 41 (4) (2001) 657–660, https://doi.org/10.1021/ ie0104262.
- [57] Marczewski, M., Kamińska, E., Marczewska, H., Godek, M., Rokicki, G., Sokołowski, G., Catalytic decomposition of polystyrenen. The role of acid and basis active centers, Appl. Catal. B Environ., 129, 236-246, doi.org/10.1016/j. apcatb.2012.09.027.
- [58] M. Beltrán, A. Marcilla, Fourier transform infrared spectroscopy applied to the study of PVC decomposition, Eur. Polym. J. 33 (1997) 1135–1142, https://doi.org/ 10.1016/s0014-3057(97)00001-3.
- [59] H.M. Zhu, X.G. Jiang, J.H. Yan, Y. Chi, K.F. Cen, TG-FTIR analysis of PVC thermal degradation and hcl removal, J. Anal. Appl. Pyrol. 82 (2008) 1–9, https://doi.org/ 10.1016/j.jaap.2007.11.011.
- [60] G. Wypych, PVC Degradation and Stabilization, CHEM TEC Publishing, Canada, 2020
- [61] X. Chen, Y. Luo, X. Bai, Upcycling polyamide containing post-consumer tetra pak carton packaging to valuable chemicals and recyclable polymer, Waste Manag. 131 (2021) 423–432, https://doi.org/10.1016/j.wasman.2021.06.031.

- [62] A.T. Hoang, S. Nižetić, X.Q. Duong, L. Rowinski, X.P. Nguyen, Advanced super-hydrophobic polymer-based porous absorbents for the treatment of oil-polluted water, Chemosphere 277 (2021), 130274, https://doi.org/10.1016/j.chemosphere.2021.130274.
- [63] K.Y. Yap, M.C. Tan, Oil adsorption onto different types of microplastic in synthetic seawater, Environ. Technol. Innovat. 24 (2021), 101994, https://doi.org/10.1016/ i.eti.2021.101994.
- [64] S.-J. Choi, T.-H. Kwon, H. Im, D.-I. Moon, D.J. Baek, M.-L. Seol, J.P. Duarte, Y.-K. Choi, A polydimethylsiloxane (PDMS) sponge for the selective absorption of oil from water, ACS Appl. Mater. Interfaces 3 (2011) 4552–4556, https://doi.org/10.1021/amp201352w.
- [65] C. Xia, Y. Li, T. Fei, W. Gong, Facile one-pot synthesis of superhydrophobic reduced graphene oxide-coated polyurethane sponge at the presence of ethanol for oilwater separation, Chem. Eng. J. 345 (2018) 648–658, https://doi.org/10.1016/j. cci. 2018.01.070.
- [66] N.H. Abd-Aziz, S. Alias, N.A. Bashar, A. Amir, S. Abdul-Talib, C.C. Tay, A short review: potential use of plastic waste as adsorbent for various pollutants, in: 6TH INTERNATIONAL CONFERENCE ON ENVIRONMENT (ICENV2018), Empowering Environment and Sustainable Engineering Nexus Through Green Technology, 2019, https://doi.org/10.1063/1.5117094.
- [67] Y. Huang, T. Gancheva, B.D. Favis, A. Abidli, J. Wang, C.B. Park, Hydrophobic porous polypropylene with hierarchical structures for ultrafast and highly selective oil/water separation, ACS Appl. Mater. Interfaces 13 (2021) 16859–16868, https://doi.org/10.1021/acsami.0c21852.